

# Lattice Distortion Oriented Angular Self-Assembly of Monolayer Titania Sheets

Yong Wang,<sup>†,||,⊥</sup> Chenghua Sun,<sup>†,⊥</sup> Xiaoxia Yan,<sup>§</sup> Faxian Xiu,<sup>||</sup> Lianzhou Wang,<sup>§</sup> Sean C. Smith,<sup>\*,†</sup> Kang L. Wang,<sup>||</sup> Gao Qing (Max) Lu,<sup>§</sup> and Jin Zou<sup>\*,†</sup>

<sup>†</sup>Materials Engineering and Centre for Microscopy and Microanalysis, <sup>‡</sup>Centre for Computational Molecular Science, AIBN, <sup>§</sup>Chemical Engineering and ARC Centre of Excellence for Functional Nanomaterials, The University of Queensland, St. Lucia, QLD 4072, Australia

<sup>||</sup>Department of Electrical Engineering, University of California at Los Angeles, California 90095, United States

**S** Supporting Information

**ABSTRACT:** Self-assembly of exfoliated monolayer titania sheets is investigated by detailed transmission electron microscopy and the force field calculations. It is demonstrated for the first time that slight but significant lattice distortions result in modified angular self-assembly of exfoliated monolayer  $\text{Ti}_{0.87}\text{O}_2$  sheets. These findings significantly broaden current knowledge of the self-assembly of exfoliated nanoscale layered sheets, which may render the potential manipulation of self-assembly of nanosheets.

In the past few years, considerable attention has been focused on two-dimensional (2D) monolayer sheets comprising one atomic or molecular layer, for example, graphene<sup>1</sup> and titania nanosheets,<sup>2</sup> due to their unique structural and physiochemical properties. These monolayer sheets, acting as a building block, can be employed to design multifunctional nanostructures with well controlled architectures.<sup>3</sup> Recently, through a layer-by-layer self-assembly approach, the fabrication of ultrathin films from exfoliated nanosheets has received significant attention.<sup>4</sup> This technique, initially designed for the multilayer assembly of polymers,<sup>3b</sup> can assemble different nanosheets into an ultrathin film with a desired thickness and a well-tailored architecture at a nanometer scale.<sup>4b,c,5</sup> Although various restacked nanofilms from nanosheets with attractive properties have been fabricated along the film normal,<sup>4,5</sup> the fundamental understanding of how the stacked nanosheets match plane by plane and what kind of crystallographic relationships might exist between the adjacent sheets is limited, mainly due to the lack of elaborate structural characterization.

Nanosheets can normally be obtained by exfoliation from the layered bulk material by soft chemical methods.<sup>2</sup> Being exfoliated from the host crystallites, the sheets may present different structural properties due to the fact that a large proportion of the atoms are now presented at the surface, as opposed to being confined within the bulk. For instance, graphene has been found not to be flat, but rather exhibits intrinsic microscopic corrugations/ripples out of the 2D plane.<sup>1</sup> Extensive studies have been made of titania nanosheets in terms of synthesis and diffraction of single sheets.<sup>2</sup> Recently, large-scale high quality titania sheets (up to 100  $\mu\text{m}$ ) were successfully synthesized, offering a reliable platform to study the structure of the exfoliated titania

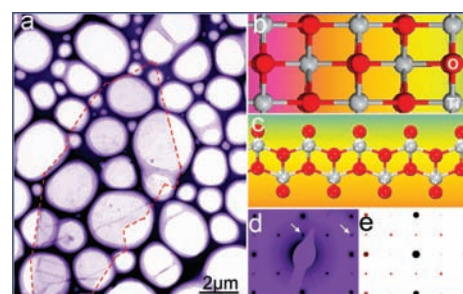


**Figure 1.** (a) A typical TEM image of a large piece of monolayer  $\text{Ti}_{0.87}\text{O}_2$  sheets (marked by dashed line). Schematic atomic models of  $\text{TiO}_2$  sheets with a 2D unit cell, from top view (b) and from the side view (c). (d) Diffraction pattern from an individual sheet and (e) simulated diffraction pattern based on a distortion model.

nanosheets. Structural modification of the exfoliated  $\text{Ti}_{0.87}\text{O}_2$  sheets has been suggested on the basis of diffraction results.<sup>2b</sup> However, the nature of this structural modification, whether it is intrinsic and how it occurs, remains unclear. More detailed attention to these structural properties is a crucial step toward useful exploitation of the 2D nanostructures.

Here, we report the first evidence that self-assembly mediated restacking of delaminated monolayer  $\text{Ti}_{0.87}\text{O}_2$  sheets does not result in randomly orientation but rather shows a particular angular stacking, caused by slight but significant structural modifications.

$\text{Ti}_{0.87}\text{O}_2$  monolayer sheets were synthesized following a well established wet-chemical procedure of exfoliating layered titanium oxide compound.<sup>2b,c</sup> The restacking was realized by adding a small amount of HCl solution to the suspension of  $\text{Ti}_{0.87}\text{O}_2$  nanosheets. Transmission electron microscopy (TEM) was performed on a FEI Tecnai 12 TEM operating at 100 kV and a Tecnai F30 TEM working at 300 kV. For simplification, we only focus on the samples with two stacking sheets.

A typical TEM image of the exfoliated titania nanosheets is shown in Figure 1a, where a large piece of nanosheet (with some debris in the bottom part) can be seen with weak but uniform contrast (marked by dashed line). Note that much better contrast of several stacked nanosheets can be found in Figure S1. Figure 1b shows the atomic models of an ideal single titania

**Received:** October 15, 2010

**Published:** December 23, 2010

sheet, viewed from the top. As reported in ref 2b, the ideal titania layer in its host layered crystallites has a 2D orthogonal unit cell with a lattice parameter of  $a = 0.3821$  nm and  $c = 0.2974$  nm. From the side view (Figure 1c), the ideal titania sheet has 4 (horizontal) atomic layers of  $\sim 0.7$  nm in thickness with two outside oxygen layers,<sup>6</sup> consistent with our TEM result (see Figure S1 and the detailed atomic coordinates in Table S1 in the Supporting Information). Figure 1d shows a typical selected area electron diffraction (SAED) pattern taken from a nanosheet. Strong and symmetric diffraction spots indicate a good crystallinity of these nanosheets. Carefully analyzing Figure 1d, we note that, other than primary strong spots, additional weak spots (arrowed) appeared in the SAED pattern, which should not originate from ideal titania nanosheets (refer to simulated diffraction pattern in Figure S2a).<sup>6</sup> The appearance of these extra diffraction spots suggests that the structure of the exfoliated sheets have been modified.<sup>2b</sup> Indeed, careful examination reveals that the unit cell based on Figure 1d is distorted (with  $a/c \sim 1.27$ ) when compared with the ideal  $\text{TiO}_2$  layer ( $a/c = 1.2848$ ).<sup>2b</sup> Our extensive TEM investigations show that most of the exfoliated sheets are in fact distorted. However, the lattice distortion is normally below 5% compared to the ideal structure.

To understand the self-assembly of the nanosheets, it is essential to clarify the structural distortion of individual sheets. As reported in a previous study, two possible factors could result in the observed weak diffraction spots.<sup>7</sup> (1) Oxygen vacancies (usually occurring in oxide materials and responsible for ordered structures in some cases).<sup>7</sup> Considering that  $\text{Ti}_{0.87}\text{O}_2$  sheets are with Ti vacancies, oxygen vacancies might not be available in the system; moreover, the possibility of oxygen vacancies is simulated and can be excluded [refer to Figure S2]. (2) Distortion of the  $\text{TiO}_6$  octahedra within the nanosheets.<sup>7a</sup> Extensive simulations are conducted through modifying the atomic coordinates of Ti and O within the unit cell. One of the examples is displayed in Figure 1e (refer to Table S1), which matches well with the experimental result in Figure 1d, indicating that the extra weak spots in the SAED patterns are indeed induced by the distortion of the  $\text{TiO}_6$  octahedra. This is consistent with the lattice distortion found in the SAED patterns (e.g., Figure 1d). Previously, Lindan and Zhang<sup>8</sup> reported that water adsorption on the (101) surface of rutile  $\text{TiO}_2$  can lead to the deformation of  $\text{TiO}_2$  substrates. In our case, however, no water is present, and thus, the observed distortion of the  $\text{Ti}_{0.87}\text{O}_2$  lattice may be the result of deviations from an ideal  $\text{TiO}_2$  monolayer, such as the edging effect and titanium vacancies.

Now the question is how such distorted nanosheets would affect the restacking of nanosheets. To answer this question, we examined hundreds of restacking of two separate nanosheets using SAED to explore their in-plane crystallographic relationships, since SAED is a powerful technique in determining the epitaxial relationship between substrates and epitaxial thin films.<sup>9</sup> Three typical examples are shown in Figure 2a–c (see Figure S3 for more examples). From these SAED patterns, two sets of diffraction spots can be, respectively, indexed by  $\text{Ti}_{0.87}\text{O}_2$  nanosheets, indicating that two sheets were indeed stacked. As marked in SAED patterns, each case has a different rotation angle corresponding to a difference between the  $a/c$  ratios of the two stacked nanosheets. To gain an overall understanding of this phenomenon, the results of about 100 samples are summarized in Figure 2d, where the rotation angle is plotted as a function of the difference of the  $a/c$  ratios. From this linear relationship, it is

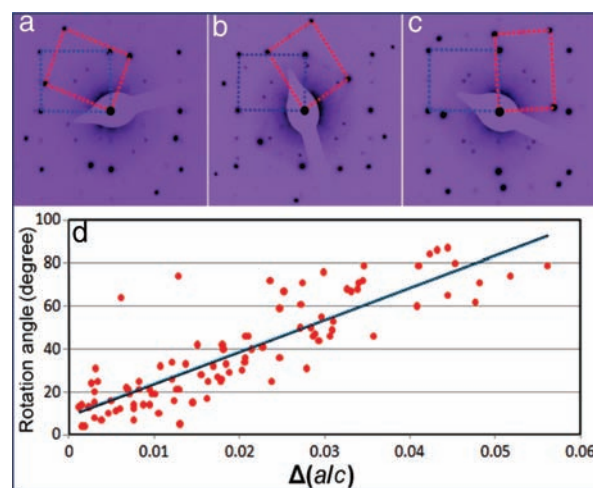


**Figure 2.** Three SAED patterns acquired from the restacked sheets with two monolayer  $\text{TiO}_2$  nanosheets, having different rotation angles: (a) 21°; (b) 55°; (c) 86°. (d) Statistic data showing the relationship between the rotation angle and the difference of the ratios of  $a/c$ .

evident that the higher the difference of the  $a/c$  ratios, the larger the rotation angle between the two stacked sheets.

It is not surprising that different stacking angles are obtained given such stacking is mainly determined by the interlayer interaction. Figure 3a shows the schematic stacking of two titania half monolayer sheets (marked as A and B), with Ti and O atoms indicated as gray and red spheres, respectively. The O–O distance within the layer corresponds to the lattice parameter of  $a$  in the unit cell. In Figure 3a, the lattice parameters of the layer A are exactly the same as the layer B (i.e., no distortion), and thus, titanium/oxygen atoms in the layer A are exactly on the top of oxygen/titanium atoms of the layer B, governed by the interlayer van der Waals interaction. In contrast, in Figure 3b, the lattice parameter  $a$  (O–O distance) is slightly reduced in level A, while level B remains unchanged. As a result, oxygen/titanium atoms in level A will deviate from their equilibrium sites shown in Figure 3a. For instance, some oxygen atoms in level A may arrive at the top site of oxygen in level B, which is not stable due to the repulsive interactions (refer to the sum of the green arrows) between two nearby oxygen atoms. Given that the repulsion force is no longer along the  $z$  direction, it cannot be fully released solely through a shift along the  $z$  direction. Consequently, the orientation angle between the layers A and B has to be adjusted, as observed in Figure 2. To reproduce this effect, force field calculations were employed to evaluate the orientated angle for two  $\text{TiO}_2$  nanosheets; computational methods can be found in the Supporting Information. In the calculation, the bottom layer is fixed and the upper layer was allowed to rotate along the layer normal, which generates the energy profile for two  $\text{TiO}_2$  nanosheets with a particular  $\Delta(a/c) \neq 0$ . As shown in Figure 3c, the optimized orientation angle is 30° when  $\Delta(a/c) = 0.0275$ , rather than 0° as in the case of  $\Delta(a/c) = 0$ , qualitatively confirming that lattice distortion can result orientation changes as revealed in Figure 2. However, if one needs to quantitatively correlate the calculation value with the experimental result, other factors, such as the edge effect and Ti vacancies, should be carefully considered.

In conclusion, through a combination of systematic TEM investigation and force field calculations, we demonstrate that delaminated monolayer  $\text{Ti}_{0.87}\text{O}_2$  sheets are not randomly

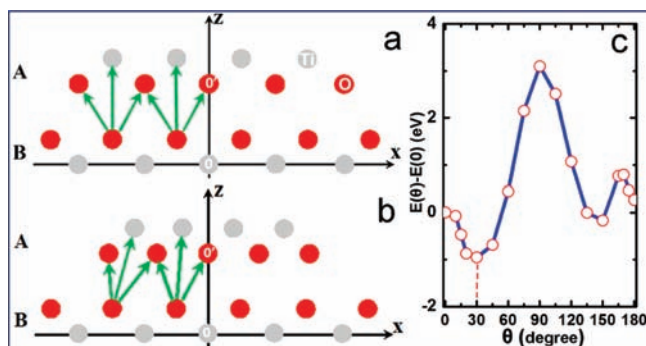


**Figure 3.** Schematic stacking of two TiO<sub>2</sub> half-nanosheets without (a) and with (b) lattice distortion. (c) Energy difference for different rotation angles for the system of two stacking sheets with  $\Delta(a/c) = 0.0275$ .

distributed in-plane when they restack, but rather demonstrate a pattern of angular stacking that is impacted by slight but significant structural modifications. It is anticipated that this finding should be a common phenomenon for exfoliated ultrathin nanosheets. The present study of titania monolayer sheets significantly advances insights into the self-assembly of exfoliated ultrathin layered sheets, shedding light on a possible route toward practical control of the self-assembly of exfoliated ultrathin layered sheets.

## ■ ASSOCIATED CONTENT

**Supporting Information.** Synthesis of monolayer Ti<sub>0.87</sub>O<sub>2</sub> sheets; TEM result of restacked sheets; more SAED patterns of two restacked sheets and computational details. This material is available free of charge via the Internet at <http://pubs.acs.org>.

## ■ AUTHOR INFORMATION

### Corresponding Author

[j.zou@uq.edu.au](mailto:j.zou@uq.edu.au); [s.smith@uq.edu.au](mailto:s.smith@uq.edu.au)

### Author Contributions

<sup>†</sup>These authors contributed equally.

## ■ ACKNOWLEDGMENT

We are thankful to the Australia Research Council, Queensland Government through Smart Future Fellowship (C.S.) and International Fellowship (Y.W.), Western Institute of Nanoelectronics (WIN) and Center on Functional Engineered Nano Architectonics (FENA), University of California at Los Angeles and the University of Queensland Research Excellence Awards (Y.W., C.S) for financial supports of this project.

## ■ REFERENCES

- (1) (a) Geim, A. K.; Novoselov, K. S. *Nat. Mater.* **2007**, *6*, 183. (b) Fasolino, A.; Los, J. H.; Katsnelson, M. I. *Nat. Mater.* **2007**, *6*, 858. (c) Berger, C.; Song, Z.; Li, X.; Wu, X.; Brown, N.; Naud, C.; Mayou, D.; Li, T.; Hass, J.; Marchenkov, A. N.; Conrad, E. H.; First, P. N.; de Heer, W. A. *Science* **2006**, *312*, 1191.
- (2) (a) Sasaki, T.; Watanabe, M.; Hashizume, H.; Yamada, H.; Nakazawa, H. *J. Am. Chem. Soc.* **1996**, *118*, 8329. (b) Tanaka, T.; Ebina, Y.; Takada, K.; Kurashima, K.; Sasaki, T. *Chem. Mater.* **2003**, *15*, 3564. (c) Osada, M.; Ebina, Y.; Funakubo, H.; Yokoyama, S.; Kiguchi,

T.; Takada, K.; Sasaki, T. *Adv. Mater.* **2006**, *18*, 1023. (d) Liu, G.; Yang, H. G.; Wang, X.; Cheng, L.; Pan, J.; Lu, G. Q.; Cheng, H.-M. *J. Am. Chem. Soc.* **2009**, *131*, 12868.

(3) (a) Keller, S. W.; Kim, H.-N.; Mallouk, T. E. *J. Am. Chem. Soc.* **1994**, *116*, 8817. (b) Decher, G. *Science* **1997**, *277*, 1232. (c) Caruso, F.; Mohwald, H. *J. Am. Chem. Soc.* **1999**, *121*, 6039. (d) Osada, M.; Sasaki, T. *J. Mater. Chem.* **2009**, *19*, 2503.

(4) (a) Fang, M. M.; Kim, C. H.; Saupe, G. B.; Kim, H. N.; Waraksa, C. C.; Miwa, T.; Fujishima, A.; Mallouk, T. E. *Chem. Mater.* **1999**, *11*, 1526. (b) Sasaki, T.; Ebina, Y.; Tanaka, T.; Harada, M.; Watanabe, M.; Decher, G. *Chem. Mater.* **2001**, *13*, 4661. (c) Tanaka, T.; Fukuda, K.; Ebina, Y.; Takada, K.; Sasaki, T. *Adv. Mater.* **2004**, *16*, 872.

(5) (a) Wang, L. Z.; Omomo, Y.; Sakai, N.; Fukuda, K.; Nakai, I.; Ebina, Y.; Takada, K.; Watanabe, M.; Sasaki, T. *Chem. Mater.* **2003**, *15*, 2873. (b) Yang, X. J.; Makita, Y.; Liu, Z. H.; Sakane, K.; Ooi, K. *Chem. Mater.* **2004**, *16*, 5581.

(6) (a) Sasaki, T.; Ebina, Y.; Kitami, Y.; Watanabe, M.; Oikawa, T. *J. Phys. Chem. B* **2001**, *105*, 6116. (b) Ma, R.; Sasaki, T. *Adv. Mater.* **2010**, *22*, 5082.

(7) (a) Xu, F. F.; Bando, Y.; Ebina, Y.; Sasaki, T. *Philos. Mag. A* **2002**, *82*, 2655. (b) Wang, Y.; Sun, C.; Zou, J.; Wang, L.; Smith, S.; Lu, G. Q.; Cockayne, D. J. H. *Phys. Rev. B* **2010**, *81*, 081401.

(8) Lindan, P. J. D.; Zhang, C. J. *Phys. Rev. B* **2005**, *72*, 075439.

(9) (a) Wang, Y.; Wang, X. N.; Mei, Z. X.; Du, X. L.; Zou, J.; Jia, J. F.; Xue, Q. K.; Zhang, X. N.; Zhang, Z. *J. Appl. Phys.* **2007**, *102*, 126102. (b) Wang, X. N.; Wang, Y.; Mei, Z. X.; Dong, J.; Zeng, Z. Q.; Yuan, H. T.; Zhang, T. C.; Du, X. L.; Jia, J. F.; Xue, Q. K.; Zhang, X. N.; Zhang, Z.; Li, Z. F.; Lu, W. *Appl. Phys. Lett.* **2007**, *90*, 151912.